Chinese Journal of
POLYMER SCIENCE

REVIEW

https://doi.org/10.1007/s10118-020-2354-5
Chinese J. Polym. Sci.

Melt Crystallization of Poly(butylene 2,6-naphthalate)

Qian Ding[a], Michelina Soccio[b], Nadia Lotti[b], Dario Cavallo[c*], and René Androsch[d*]

[a] *School of Packaging Design and Art, Hunan University of Technology, Zhuzhou 412007, China*
[b] *Department of Civil, Chemical, Environmental and Materials Engineering, University of Bologna, Via Terracini 28, Bologna 40131, Italy*
[c] *Department of Chemistry and Industrial Chemistry, University of Genova, Via Dodecaneso 31, Genova 16146, Italy*
[d] *Interdisciplinary Center for Transfer-oriented Research in Natural Sciences (IWE TFN), Martin Luther University Halle-Wittenberg, Halle/Saale 06099, Germany*

Abstract Poly(butylene 2,6-naphthalate) (PBN) is a crystallizable linear polyester containing a rigid naphthalene unit and flexible methylene spacer in the chemical repeat unit. Polymeric materials made of PBN exhibit excellent anti-abrasion and low friction properties, superior chemical resistance, and outstanding gas barrier characteristics. Many of the properties rely on the presence of crystals and the formation of a semicrystalline morphology. To develop specific crystal structures and morphologies during cooling the melt, precise information about the melt-crystallization process is required. This review article summarizes the current knowledge about the temperature-controlled crystal polymorphism of PBN. At rather low supercooling of the melt, with decreasing crystallization temperature, β'- and α-crystals grow directly from the melt and organize in largely different spherulitic superstructures. Formation of α-crystals at high supercooling may also proceed *via* intermediate formation of a transient monotropic liquid crystalline structure, then yielding a non-spherulitic semicrystalline morphology. Crystallization of PBN is rather fast since its suppression requires cooling the melt at a rate higher than 6000 K·s^{-1}. For this reason, investigation of the two-step crystallization process at low temperatures requires application of sophisticated experimental tools. These include temperature-resolved X-ray scattering techniques using fast detectors and synchrotron-based X-rays and fast scanning chip calorimetry. Fast scanning chip calorimetry allows freezing the transient liquid-crystalline structure before its conversion into α-crystals, by fast cooling to below its glass transition temperature. Subsequent analysis using polarized-light optical microscopy reveals its texture and X-ray scattering confirms the smectic arrangement of the mesogens. The combination of a large variety of experimental techniques allows obtaining a complete picture about crystallization of PBN in the entire range of melt-supercoolings down to the glass transition, including quantitative data about the crystallization kinetics, semicrystalline morphologies at the micrometer length scale, as well as nanoscale X-ray structure information.

Keywords Poly(butylene 2,6-naphthalate); Crystallization; Polymorphism; Semicrystalline morphology

Citation: Ding, Q.; Soccio, M.; Lotti, N.; Cavallo, D.; Androsch, R. Melt crystallization of poly(butylene 2,6-naphthalate). *Chinese J. Polym. Sci.* https://doi.org/10.1007/s10118-020-2354-5

INTRODUCTION

Poly(butylene 2,6-naphthalate) (PBN) is a high-performance aromatic polyester resin. It is generally obtained by polycondensation of 1,4-butanediol and dimethyl 2,6-naphthalate. The use of dimethyl 2,6-naphthalate is preferred over 2,6-naphthalene dicarboxylic acid, since it allows to operate in milder reaction conditions. In fact, the diester is characterized by lower melting temperature than the diacid, and methanol (CH_3OH), produced in the first step of the synthesis, is a better leaving group than H_2O molecule. Polycondensation is carried out in bulk involving two main steps: the first in an inert atmosphere at a temperature between 200 and 230 °C and the second under vacuum at higher temperature (up to 260 °C). An excess (from 20% to 100%) of diol with respect to the diester (or diacid) is generally used. Ti-based catalysts, in particular tetrabutyl titanate and titanium isopropoxide, are mainly employed.[1–3] Another synthesis strategy used to obtain PBN with an inherent viscosity lower than that of commercial grades is ring-opening polymerization. Nevertheless, this procedure is still conducted at high temperature (275 °C) and involves the use of 2,6-naphthalenedicarbonyl dichloride, with release of HCl, and dichloromethane as solvent.[4]

The chemical structure of PBN, shown in Fig. 1, provides excellent chemical resistance to most organic solvents, acids and bases, reducing and oxidizing agents. Moreover, PBN exhibits high thermal resistance, very good mechanical behavior both in terms of resistance and wear, and outstanding barrier performance against gas and water vapor.[1,3,5,6] It is worth noting that all the properties mentioned are better than those of the corresponding terephthalate-based counterpart poly(butylene terephthalate) (PBT).

The presence of rigid aromatic sub-units along the macromolecular backbone, such as the naphthalene ring, consistently stiffens the polymer chains, resulting in a high glass transition temperature (T_g) of 78 °C. PBT, whose T_g is around

* Corresponding authors, E-mail: dario.cavallo@unige.it (D.C.)
E-mail: rene.androsch@iw.uni-halle.de (R.A.)

Invited review
Received July 14, 2019; Accepted September 4, 2019; Published online November 15, 2019

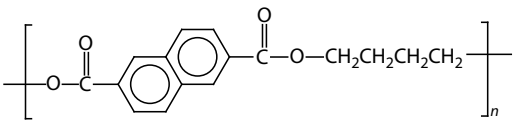

Fig. 1 The chemical structure of PBN.

room temperature, turns out to be less rigid, indicating the phenyl aromatic sub-unit is characterized by a reduced stiffening effect. On the other hand, the flexible aliphatic segment (glycol moiety) of the repeating unit confers great crystallization capability to PBN, leading to the formation of crystals of very high melting temperature (T_m) up to 243 °C. These characteristics make PBN particularly suitable for applications that expose the polymer to high temperature. In fact, it is widely employed, mainly in form of fibers, in high-demanding applications, such as aerospace, electronics, and electrical engineering. In form of films, it is utilized for food packaging applications.[7,8] To tailor the functional properties towards specific applications, the neat PBN has also been modified by blending,[9–12] or copolymerization,[13–16] and is also used as matrix in nanocomposites.[17–19]

The linear chain-conformation of PBN typically leads to rather fast crystallization on cooling the melt and the formation of a semicrystalline superstructure. The maximum achievable crystallinity is around 30%, however, with the structure, morphology, and higher-order organization of crystals strongly depending on the crystallization conditions. The rather low maximum crystallinity of around 30% is in accord with the observation of a link with the chain mobility in crystals. Typically, only in polymers with highly mobile chains in the crystalline phase can high crystallinity be observed. In this review, first, the structure of the various crystal polymorphs (*α*-, *β*-, and *β*′-crystals, including a liquid crystalline mesophase) at the length-scale of the unit cell as well as selected thermodynamic properties (bulk specific enthalpy of melting and equilibrium melting temperature) are summarized. Secondly, the crystallization processes at low and high supercooling of the melt are described in detail, accounting for the qualitatively different nucleation and growth pathways the melt transforms into crystals. At high supercooling of the melt, crystallization proceeds *via* intermediate formation of a liquid crystalline mesophase, following Ostwald's rule of stages. This behavior is similar to other polyesters which contain a mesogenic unit in the main chain, briefly commented in particular regarding the structure of the mesophase. Besides detailed information about the kinetics of the phase transformations, the discussion of PBN crystallization at low and high supercooling of the melt also includes important information about the semicrystalline morphology at the micrometer-length scale. Thirdly, the suppression of crystallization and ordering processes during cooling and the condition of full vitrification of the melt are also summarized. On heating the obtained glass to above the glass transition temperature cold-crystallization may occur, as described in the same section.

STRUCTURE OF CRYSTAL POLYMORPHS AND OF THE LIQUID CRYSTALLINE MESOPHASE AT THE NANOSCALE

Similar to the analogue polymer with a single aromatic rings, PBT,[20] two main crystalline polymorphs have been reported for PBN as well. [21,22] Next to the crystalline *α*-form, which crystallizes from the melt under conventional conditions, a different polymorph, the *β*-form, has been found upon uniaxial drawing of PBN films. Further studies demonstrated that the polymorphs can both be obtained by melt crystallization,[23,24] depending on the applied cooling rate or isothermal crystallization temperature, as later discussed in this review. Melt-crystallized *β*-form is typically indicated as *β*′-phase.

The two crystalline structures have been resolved, thanks to the obtainment of fiber diffraction patterns in drawn samples. Both polymorphs display triclinic unit cells, which contain a single repeat unit.[21,22] A schematic view of chain packing along different crystallographic directions is shown in Fig. 2, together with a summary of the structural parameters of the two unit cells. The *β*-polymorph exhibits a higher density with respect to the *α*-form, that is, 1.39 versus 1.36 g·cm^{-3}. From Fig. 2, it can be deduced that the molecular packing of the *α*- and *β*-forms is very similar and that the major difference is the conformation of the butylene sub-unit. Such "slight distortion" of crystalline structure is also observed in other polymers, such as poly(L-lactic acid) (*α*- and *α*′-form), as well as PBT (*α*- and *β*-form). However, in the case of isotactic polypropylene, as well as many polyamides, mesophases forming at high supercooling of melt may not be clas-

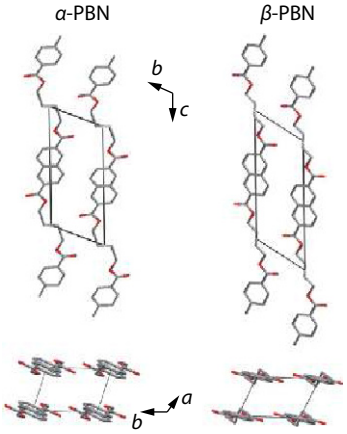

Crystal form	*α*-form	*β*′-form
Crystal system	Triclinic	Triclinic
Space group	$P\bar{1}$	$P\bar{1}$
Density (g·cm^{-3})	1.36	1.39
T_m^0 (°C)	261	281
Cell parameters		
a (nm)	0.487	0.455
b (nm)	0.622	0.643
c (nm)	1.436	1.531
α (deg)	110.78	110.1
β (deg)	126.90	121.1
γ (deg)	97.93	100.6

Fig. 2 Arrangement of the polymer chains in *α*-form (left) and *β*-form (right) of PBN: view along the *a*-axis (top) and a projection along the *c*-axis (bottom). (Adapted with permission from Ref. [19]; Copyright (2010) Elsevier.)

https://doi.org/10.1007/s10118-020-2354-5

sified as "slightly distorted" since often only pseudo-hexagonal symmetry is achieved, that is, just an isotropic lateral correlation between chains.

On the basis of infrared spectra and solid-state ^{13}C-NMR, the main difference between the two crystal structures has been proposed to be related to the conformation of the glycol residue, that is, with a more extended *trans*-planar conformation of both the ester and the methylene groups characterizing the β-form. The conformation of the ester and glycolic methylenes in the α-phase is instead S'G'TGS.[22,25] On the other hand, other authors provided an alternative view on the conformational differences, pointing instead to a larger degree of coplanarity between the ester groups and the naphthyl rings in the β-form, with respect to the α-polymorph.[24,26] As a consequence of this increased planarity, a tighter packing of the polymer chains in the β-form unit cell is possible, resulting in its higher density. Recent density functional theory calculations have confirmed that both these features, that is, *trans*-planar conformation of the methylene segment and larger coplanarity of the ester groups and naphthalene rings, are distinctive for the β-form.[27]

For what concerns the thermodynamic properties, the equilibrium melting temperature was obtained for both polymorphs, exploiting a copolymerization strategy which enabled to promote β-form crystallization.[28] By proper modelling of the equilibrium melting temperature variation with comonomer content, T_m for the two polymorphs in the homopolymer could be obtained. Values of 261 and 281 °C were found for the α- and β-forms, respectively.[28] This result is in agreement with the experimentally observed faster formation kinetics of the β-form at high temperatures. A bulk enthalpy of melting of 122 J·g^{-1} is reported for the α-form,[29] while a higher value is expected for the β-phase,[23] though an exact determination is lacking. It is in fact difficult to prepare samples of different crystalline/amorphous ratios due to the high crystallization rate of PBN.

Besides the three crystal polymorphs described above, PBN forms a mesophase at high supercooling of the melt, discovered on quenching the melt to 0 °C, and bypassing the temperature-range of fast crystallization at higher temperature.[30] Fig. 3 shows in the bottom graph X-ray diffraction (XRD) patterns of PBN crystallized at 180 °C (top curve), of quenched PBN containing the mesophase (center curve), and of the melt of PBN at 255 °C (bottom curve). The XRD curve of quenched PBN is distinctly different from that of the melt or observed after crystallization, such that there is detected a weak though sharp peak at a position corresponding to a repeat distance of 14.3 Å (see blue arrow), and a broad halo superimposed by shoulder peaks. X-ray fiber pattern obtained on quenched and subsequently stretched PBN, shown in the top part of Fig. 3, allowed further interpretation of the origin of the low-angle 14.3 Å peak and higher-angle shoulder peaks, being located at the meridian and equator, respectively. As the meridian is parallel to the stretching direction, the sharp low-angle peak reveals crystal-like periodicity along the chain axis while the broad equatorial scattering maxima indicate liquid-like lateral, interchain correlations. Moreover, the absent splitting of meridional and equatorial maxima in the fiber pattern suggest the formation of a smectic A (SA)

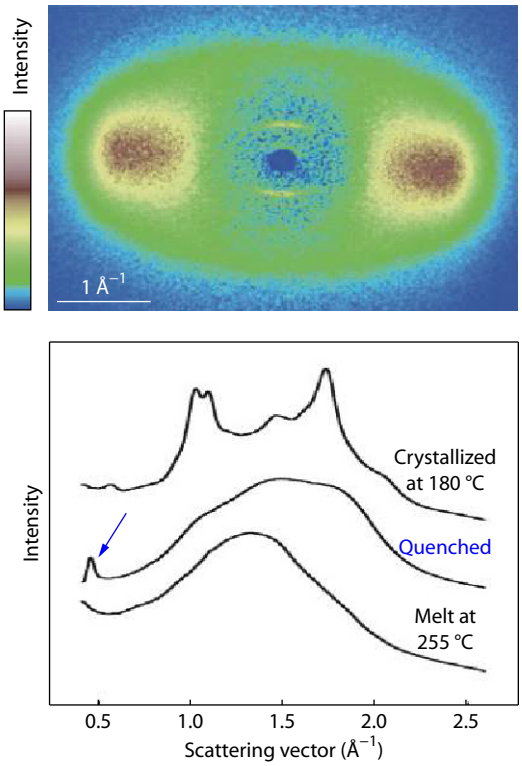

Fig. 3 Bottom: XRD patterns obtained on PBN of different thermal histories. Samples were subject to crystallization at 180 °C, quenching to 0 °C, or melting at 255 °C, as indicated at the various curves. Top: an X-ray fiber pattern obtained on initially quenched and then stretched PBN. The stretching direction is parallel to the meridional direction in the image. (Adapted with permission from Ref. [30]; Copyright (2008) American Chemical Society.)

phase,[31] in which bundles of mesogenic groups form stacked layers, with the basal planes of these layers oriented perpendicularly to the stretching direction. At room temperature, the mesophase of PBN is frozen and therefore considered as a liquid crystal glass (LC glass).[32,33] Comparison of the fiber repeat distance of the PBN LC glass with that of the α-crystal form suggests that the local chain conformations are similar in both structures.

CRYSTALLIZATION OF PBN AT LOW SUPERCOOLING OF THE MELT

Crystallization at low supercooling of the melt, that is, on cooling the melt at rates much lower than 10 K·min^{-1} (0.17 K·s^{-1}) or at temperatures above around 200 °C, leads to the formation of β'-crystals.[23,24,34] Growth of β'-crystals fades if the cooling rate is higher than 0.1 K·min^{-1} (0.0017 K·s^{-1}) or if the crystallization temperature decreases to values lower than 230 °C. In parallel, there is increasing formation of α-crystals. Finally, if the cooling rate is higher than 10 K·min^{-1} (0.17 K·s^{-1}) or if the temperature of crystallization is lower than about 200 °C, then only α-crystals are formed. Fig. 4 shows the dependence of crystallization temperature on the cooling rate,[34] however, with the data not revealing any hint about the change of crystal polymorph when varying the crystallization conditions in the

https://doi.org/10.1007/s10118-020-2354-5

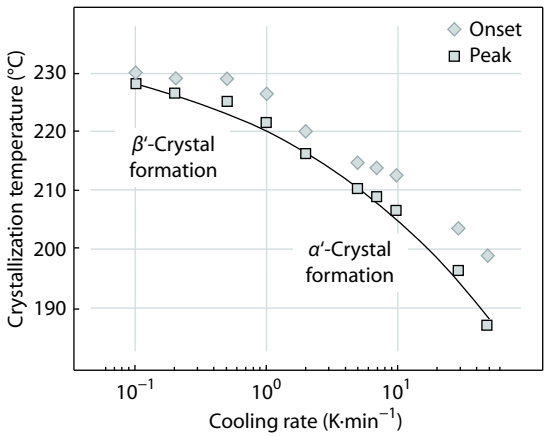

Fig. 4 Crystallization temperature of PBN as a function of the cooling rate at low supercooling of the melt. (Adapted with permission from Ref. [34]; Copyright (2001) Elsevier.)

shown range.

β'-crystals "grow radially and almost individually from the center" of dendritic spherulites,[24] with such morphology attributed to the very slow crystal growth rate, "allowing texture growth to reach the most thermodynamically stable state during crystallization."[24] For illustration, the top left image in Fig. 5 shows large β'-spherulites with long needle-like crystals radially grown from point-like nuclei into the surrounding melt during cooling at 0.1 K·min^{-1}.[24] The top right image shows α-spherulites, as they appear during isothermal crystallization at 200 °C in a polarized-light optical microscope. Though very faint, the α-spherulites show the typical Maltese cross indicating radial alignment of crystal lamellae, which can be more clearly recognized in the α-spherulites shown in the bottom right image of Fig. 5, grown at 190 °C.[35]

Direct comparison of the different spherulite morphologies forming as a function of the crystallization temperature in the low-supercooling temperature-range is provided with the bottom left image. Development of β'-spherulites was enforced by isothermal annealing the sample at 215 °C for a period of 40 min, causing the formation of dendritically grown β'-spherulites with a size of around 20 μm. Before conversion of the entire melt into a semicrystalline spherulitic structure, the remaining melt was cooled to 190 °C for continuation of crystallization and growth of α-spherulites. The largely different morphologies of β'- and α-spherulites are clearly visible.[35]

The isothermal crystallization of PBN at low supercooling of the melt was investigated using conventional DSC,[13,16,29,36] with the dependence of crystallization half-time ($t_{1/2}$) on the crystallization temperature shown in Fig. 6. It can be clearly seen that $t_{1/2}$ of PBN drastically increases with the crystallization temperature in the analysed temperature range, indicating that the overall crystallization rate of PBN decreases with decreasing supercooling. Moreover, both α- and β'-crystals are able to crystallize directly from the melt between 205 and 225 °C. As mentioned before,[28] β'-crystals are thermodynamically favored and tightly packed, while α-crystals are kinetically favored, crystallizing much faster than β'-crystals, which is confirmed by the results of isothermal crystallization experiments at low supercooling of the melt. At the crystallization temperature of 225 °C, the value of $t_{1/2}$ exceeds 10 min, connected with the pre-dominant formation of β'-crystals with an extremely low growth rate.[24] When the crystallization temperature decreases from 225 °C to 205 °C, the formation of β'-crystals is gradually replaced by the faster formation of α-crystals,[34] however, with the temperature-dependence of the half-time not showing any discontinuity.

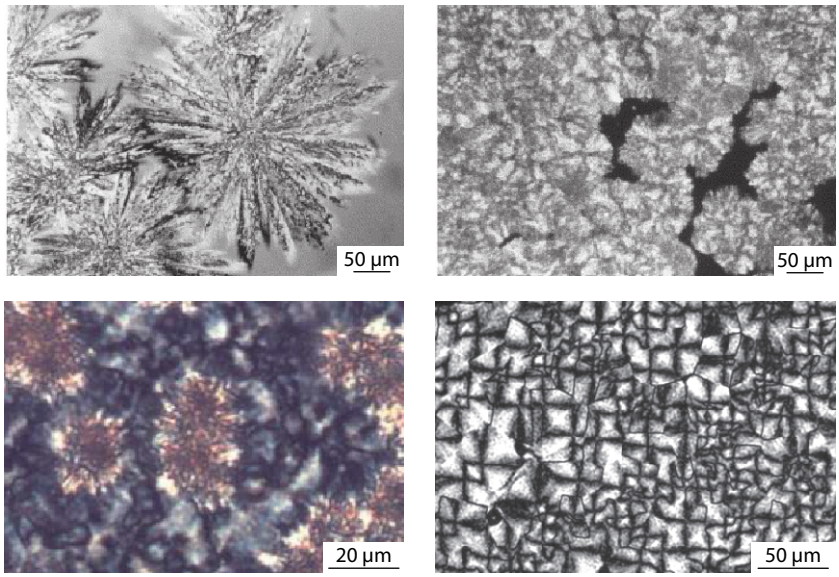

Fig. 5 POM images showing α-spherulites isothermally grown at 200 °C (top right) and β'-spherulites grown on cooling the melt at a rate of 0.1 K·min^{-1} (top left). (Adapted with permission from Ref. [24]; Copyright (2002) Elsevier) The bottom two images show α-spherulites isothermally grown at 190 °C (right) and β'-form spherulites grown at 215 °C for 40 min embedded in matrix of α-form spherulites formed at 190 °C (left). (Adapted with permission from Ref. [35]; Copyright (2018) Elsevier.)

https://doi.org/10.1007/s10118-020-2354-5

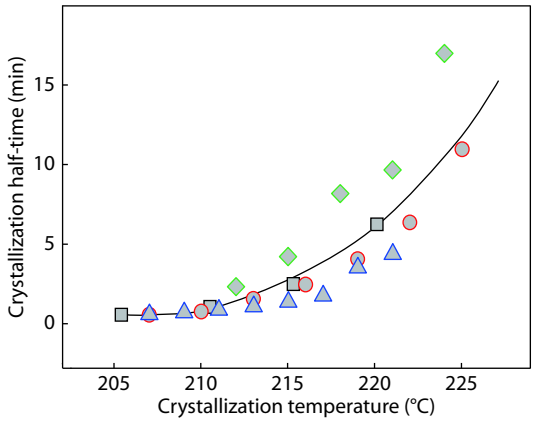

Fig. 6 Crystallization half-time of PBN as a function of the crystallization temperature. The symbols of different color and shape represent crystallization data of different sources (black squares[13], green rhombus[16], blue triangles,[29] and red circles[36]).

CRYSTALLIZATION OF PBN AT HIGH SUPERCOOLING OF THE MELT *VIA* INTERMEDIATE LIQUID CRYSTAL FORMATION

Direct formation of *α*-crystals from the melt only occurs at temperatures higher than about 160 °C. Below this temperature, crystallization proceeds according to Ostwald's rule of stages,[37,38] *via* intermediate formation of a liquid-crystalline mesophase.[35,39,40] The Ostwald's rule, which states that a phase transition proceeds *via* metastable states, whenever they exist, through stages of increasing stability, is an empirical observation widely obeyed in a variety of systems, including organic molecules,[41] inorganic compounds,[42] proteins,[43,44] and colloids.[45,46]

In particular, the crystallization behavior of PBN at high supercoolings resembles that of typical main-chain liquid crystalline polymers in which nematic or smectic mesophases, possessing orientational or both orientational and translational order of the molecular motifs, respectively, can appear as transient states on the route to the most stable crystalline structure.[32,47–50] Many examples are reported for polyesters containing aromatic mesogenic units.[51] Detailed studies on structure formation with varying molecular composition exist for polyesters derived from bibenzoic acid and oxyalkylene glycols.[32,52–57] Smectic mesophases form upon cooling the isotropic melt, and then transform into crystals upon further cooling, in polyesters of bibenzoate with diols spacers containing from three to nine methylene units.[56,57]

Of particular interest regarding the behavior of PBN is the case of poly(heptamethylene 4,4′-bibenzoate-*co*-heptamethylene terephthalate) with 10 mol%–20 mol% of a terephthalate co-unit. These thermotropic liquid-crystalline copolyesters display two crystallization modalities, that is, the formation of the stable crystalline phase can occur either directly from the isotropic melt at low supercoolings or from a smectic mesophase at lower crystallization temperatures.[49,50] Thus, the empirical Ostwald's rule of stages can both be obeyed and defeated, by a given polymer, depending on the crystallization conditions. In the field of polymer crystallization, the occurrence of Ostwald's rule of stages and the role of metastable states have been discussed in details by Keller and Cheng.[58–61] Their interpretation relies on the analysis of transition kinetics of the stable and metastable phases, and it will be briefly described, with reference to the PBN case, in the following.

On the basis of the peculiar crystallization behavior of PBN,[30,35] and in analogy with the above referred liquid-crystalline polyesters, the PBN mesomorphism can be defined as monotropic. In a monotropic system, the mesophase is metastable throughout the entire temperature range with respect to the liquid or crystalline phases, which are the ultimately stable phases above and below the crystal melting point, respectively. This situation is schematically depicted in the free enthalpy versus temperature diagram of Fig. 7, where, for the sake of simplicity, only the crystalline *α*-phase is considered.

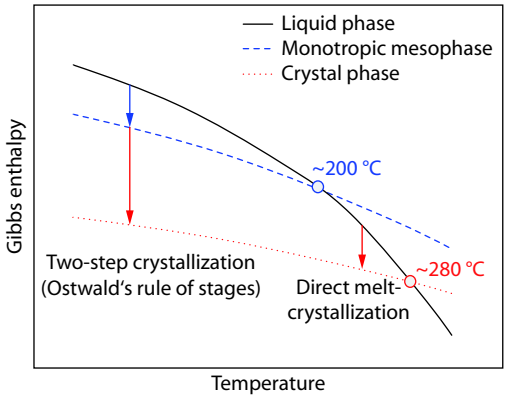

Fig. 7 Temperature-dependence of Gibbs enthalpy of the melt (black solid), of the monotropic liquid-crystalline mesophase (blue dash), and of the crystal phase (red dot). Different isothermal crystallization routes below and above the stability limit of the mesophase (blue circle) are indicated with the vertical arrows. (Adapted with permission from Ref. [39]; Copyright (2018) Elsevier.)

Clearly, two distinct crystallization behaviors can be expected. For crystallization temperatures between approximately 280 and 200 °C, that is, between the equilibrium melting point of the *α*-phase[28] and the isotropization temperature of the smectic phase,[30,40] structuring from the isotropic melt can only occur directly to the crystalline phase and the behavior predicted by Ostwald's rule cannot be observed. If melt-crystallization is bypassed, for instance by rapid cooling, a crystallization-temperature range in which the liquid-crystalline phase is also supercooled can be achieved. With increasing supercooling, the most likely situation from a kinetic perspective is an inversion between the rate of formation of the stable and metastable phases.[58] Therefore, when the rate of formation of the smectic phase from the melt becomes larger than that of melt crystallization, a two-step structuring process occurs: first a transition from the melt to the liquid-crystalline phase, which is followed by the transformation of smectic liquid crystalline mesophase into *α*-crystals, according to the Ostwald's rule of stages.

The first evidence of the two-step crystallization process at high supercooling of the melt was collected with a heating-experiment performed on initially quenched and mesophase-containing PBN.[30] Slow heating the above described meso-

phase (see Fig. 3), being in the glassy state at ambient temperature, to temperatures higher than its glass transition temperature $T_{g,LC}$ of 65 °C, caused transformation to *α*-crystals at about 80 °C. Thus, the melt first partially transformed into liquid-crystalline (LC) mesophase, then the LC-phase vitrified on continued fast cooling to below $T_{g,LC}$, and upon reheating and devitrification of the LC-glass, cold-crystallization of the mesophase occurred. Further details about the cold-crystallization behavior are provided below, in the next section.

In the initial study of the mesophase of PBN,[30] the rate of quenching, needed for its isolation and the subsequent X-ray analyses, was too high to allow completion of the crystallization process during cooling. For this reason, the kinetics of the two-step melt-crystallization process was analyzed systematically by non-isothermal and isothermal crystallization experiments. Fig. 8 shows crystallization temperatures as a function of the cooling rate,[35] providing clear evidence about different crystallization mechanisms when cooling slower or faster than about 1 K·s^{-1} to 10 K·s^{-1}. Cooling slower than 1 K·s^{-1} to 10 K·s^{-1} leads to direct transformation of the melt into *β*′- or *α*-crystals (red data points) (see also Fig. 3), with the width of transition increasing with the cooling rate, similar to that in Fig. 4. Note that the red dashed line indicates the approximate onset of crystallization, while the data points/solid lines represent peak temperatures. It is obvious that on cooling at rates between 1 and 10 K·s^{-1} crystals begin to form at high temperature, however, with the crystallization process incomplete. Crystallizable melt then transforms according to a different mechanism at around 160 °C, being dominant on cooling faster than 10 K·s^{-1}. First, at higher temperature, the melt converts into LC-mesophase (black/gray data points) which then transforms into *α*-crystals at slightly lower temperature (blue data points). However, there exists a critical cooling rate above which the transition of LC-mesophase into crystals is suppressed for kinetic reasons, being about 400 K·s^{-1}. In that case, the mesophase vitrifies at its glass transition temperature, a situation achieved in the initial quenching experiments performed to study the X-ray structure of the mesophase (see Fig. 3). Finally, if the cooling rate exceeds about 6000 K·s^{-1} then even LC-mesophase formation is inhibited (see vertical gray arrow).[40] Worth noting, despite that ordering is suppressed at such high cooling rate, avoiding nuclei formation requires even much faster cooling at rates higher than 30000 K·s^{-1} as was analyzed by the cold-crystallization behavior which allows detection of presence of nuclei;[40] more information is provided below in the section about vitrification and cold-crystallization of PBN.

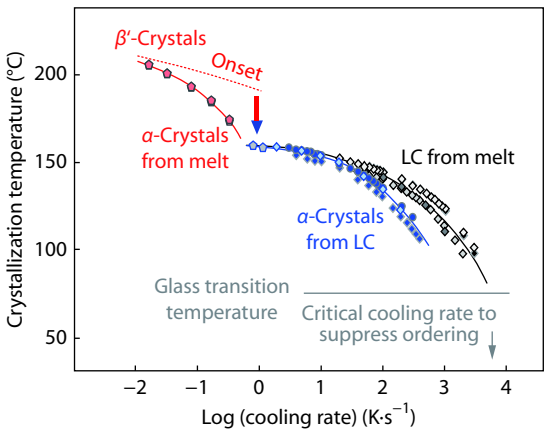

Fig. 8 Crystallization peak temperature of PBN as a function of the cooling rate, including information about the specific crystal polymorph forming either from the melt or from the LC-mesophase. The vertical arrow indicates the critical cooling rate above which the isotropic melt vitrifies without prior ordering,[40] and the horizontal line approximately represents the glass transition temperature.[30] (Adapted with permission from Ref. [35]; Copyright (2018) Elsevier.)

In order to obtain direct evidence on the two-step crystallization process, synchrotron X-ray scattering data were collected during fast cooling the melt.[62] Fig. 9 shows with the top and bottom sets of curves time-/temperature-resolved X-ray experiments, obtained during ballistic cooling of a specific PBN grade at average rates of 35 and 100 K·s^{-1}, respectively. Front curves represent data collected at high temperature and show the characteristic amorphous halo of the melt. Cooling using a rate of 35 K·s^{-1} leads to the direct formation of crystals, while during cooling at 100 K·s^{-1}, the mesophase formation precedes crystallization as recognized by the appearance of different scattering characteristics when comparing to the patterns of the melt and crystals. Referring to the data shown in Fig. 8, it can be noted that there is an apparent slight mismatch between the cooling-rate ranges in which direct melt-crystallization is obtained. This is attributed to the ballistic cooling scheme in the X-ray experiments and also the employment of different PBN grades. Regarding the latter, presence of additives, which act as heterogeneous nucleation sites in the crystallization process, shift the high-temperature crystallization event, indicated with the red data points in Fig. 8, to higher temperatures, slightly affecting the

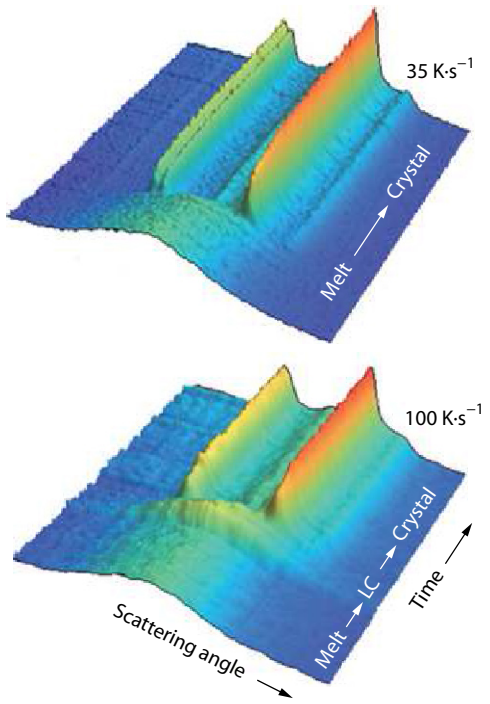

Fig. 9 Time-resolved XRD patterns during cooling PBN samples at approximately 35 and 100 K·s^{-1}. (Adapted with permission from Ref. [62]; Copyright (2012) American Chemical Society.)

https://doi.org/10.1007/s10118-020-2354-5

cooling rate at which the one-step crystallization process turns into a two-step crystallization process.

Isothermally collected crystallization data confirm the multi-stage crystallization process of PBN at high supercooling of the melt. Fig. 10(a) shows calorimetrically measured crystallization exotherms, heat-flow rate as a function of the crystallization time, after cooling the melt to different crystallization temperatures, as indicated at the right-hand side of the curves.[62] The cooling rate on the approach of the crystallization temperature was selected being sufficiently high, 1000 K·s^{-1}, to bypass the high-temperature crystallization process discussed above. The data of Fig. 10(a) reveal for all analyzed temperatures between 135 and 147 °C two exothermic peaks, which are associated to the formation of LC-mesophase from the melt and the transformation of LC-mesophase into *α*-crystals. With decreasing crystallization temperature, both transitions proceed faster (see black and blue dashed lines), being too fast to follow them at temperatures lower than about 130 °C. Note that the two-step crystallization process is complete within 1 s, which required application of fast scanning chip calorimetry (FSC)[64,65] and use of nanogram-sized samples to achieve high cooling rate and the required time-resolution for collection of heat-flow rate data, instead of conventional differential scanning calorimetry (DSC), for quantitative evaluation of the kinetics. Evidence for the assignment of two transition peaks to the formation of LC-mesophase from the melt and the crystallization of LC-mesophase was collected by interrupting the phase transitions at pre-selected times during FSC, quenching the sample to ambient temperature, and microfocus beam X-ray diffraction analysis of the phase structure, not shown (see Fig. 2 in Ref. [66]).

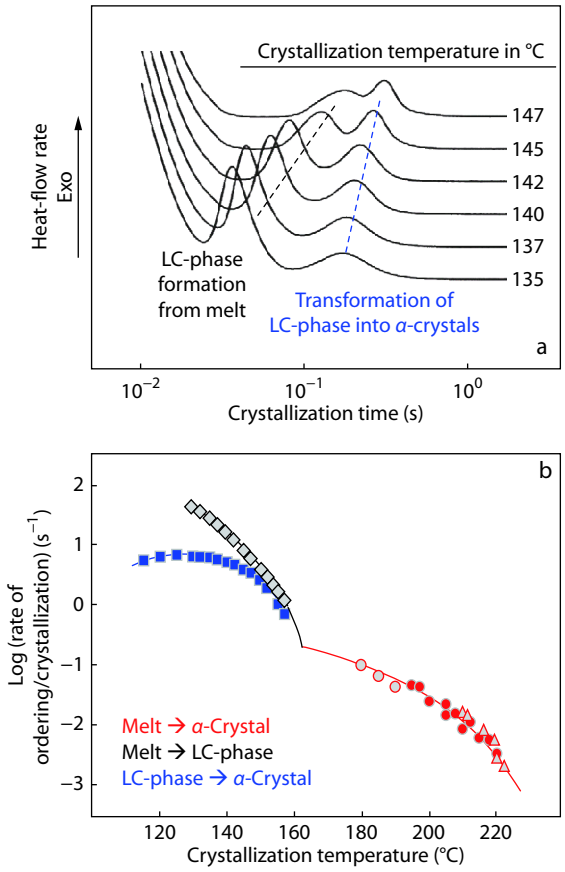

Fig. 10 (a) Heat-flow rate as a function of time during isothermal crystallization of PBN at the indicated temperatures. (b) Rate of LC-mesophase formation and of crystallization as a function of temperature. The different symbols associated to *α*-phase crystallization represent data of different sources (gray/red circles,[62] red circles,[13] triangles.[63]) (Adapted with permission from Ref. [62]; Copyright (2012) American Chemical Society.)

Fig. 10(b) provides quantitative information about the crystallization/ordering kinetics, showing the inverse peak-time of phase transitions as a function of the crystallization rate; the peak-time of ordering or crystallization is the time at the maximum heat-flow rate in FSC curves shown in Fig. 10(a), that is, the time at which the phase transition is fastest. It may be considered as an approximate of more commonly reported transition halftimes, though determination of peak-times is much more reliable. Red data points refer to direct formation of *α*-crystals from the melt, which is only evident at temperatures higher than about 160 °C. At lower temperatures, the crystallization process proceeds according to Ostwald's rule of stage *via* fast formation of the mesophase (gray diamond symbols) followed by its conversion into *α*-crystals (blue squares). Note that isothermal and non-isothermal crystallization experiments of the crystallization kinetics (Figs. 8 and 10, respectively) yielded consistent information about the crossover temperature of 160 °C where the one-stage crystallization process is replaced by the two-stage crystallization process.

Quantitative analysis of the peak areas of the crystallization isotherms allowed estimation of the enthalpy of LC-phase formation. Fig. 11 shows the two-step crystallization-isotherm measured at 150 °C, with the two slightly overlapping peaks de-convoluted to obtain the individual enthalpies of the phase transitions. The formation of LC-phase from the melt and the transition of LC-phase into crystals are gray and blue color-coded, respectively, in analogy to the data shown in Fig. 10. The percentage areas/enthalpies of these transitions amount to 22% and 78%, respectively, yielding addi-

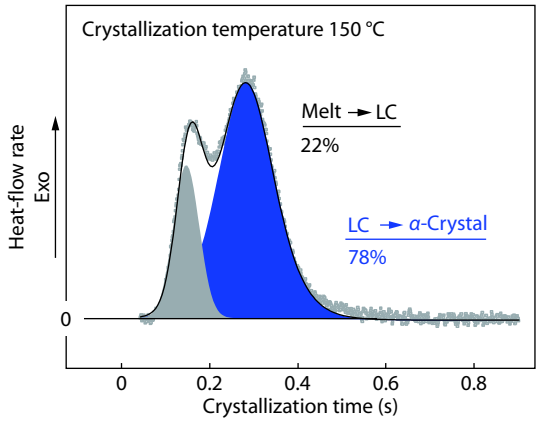

Fig. 11 Heat-flow rate as a function of time, recorded during isothermal crystallization of PBN at 150 °C, including illustration of deconvolution of individual transitions of the melt into LC-phase (gray) and of the LC-phase into *α*-crystals (blue). (Adapted with permission from Ref. [66]; Copyright (2018) Elsevier.)

https://doi.org/10.1007/s10118-020-2354-5

tional information in particular about the nature of the LC-mesophase.

The observed percentage value of the enthalpy of transforming melt into a smectic liquid crystal of roughly 20%–25% of the total crystallization enthalpy agrees with the literature.[33,67,68] Here it is reported that transforming the melt into a crystal involves an enthalpy-change of 30–50 kJ·mol^{-1} (33 kJ·mol^{-1} for PBN[13,29]) while it is only 4–6 kJ·mol^{-1} for transforming melt into a smectic liquid crystal. In the case of formation of a nematic liquid crystal from the melt, the transition enthalpy would be even lower (1–2 kJ·mol^{-1}).[68] Accordingly, the bulk enthalpy of transforming the melt into a smectic liquid crystal is around 10%–15% of the total crystallization enthalpy but only around 1%–5% when forming a nematic structure. As such, the experimental observation of a percentage enthalpy of liquid-crystal formation slightly higher than 20% of the total crystallization enthalpy serves as further evidence that in PBN a smectic but not a nematic LC structure forms as intermediate step in the crystallization process.

Polarized-light optical microscopy (POM) provides information about the morphology of PBN at the micrometer length-scale. Fig. 12 shows POM images of PBN samples prepared during FSC by cooling the melt at rates of 1, 10, 100, and 1000 K·s^{-1}, with these rates selected to identify characteristic differences as predicted by different crystallization schemes according to the data of Fig. 8.[35] Cooling PBN at 1 K·s^{-1} causes spherulitic growth of *α*-crystals directly from the melt, with the transition beginning above 200 °C (see dashed red line in Fig. 8) and stretching down to 160 °C where the remaining amorphous but crystallizable fraction converts to crystals *via* intermediate formation of the LC-mesophase. Cooling at 10 K·s^{-1} leads to a similar though finer structure due to the increased nuclei number. Similar as on cooling at 1 K·s^{-1}, the sample consists of amorphous structure and *α*-crystals, with the major crystal fraction likely formed from the LC-mesophase. Increasing the cooling rate to 100 K·s^{-1} yields a multiphase morphology containing amorphous phase, LC-mesophase, and *α*-crystals as proven by complementary X-ray analysis (not shown, see Fig. 5 in Ref. [35]). The POM image shows both Schlieren originating from the mesophase and fine grains, with the latter indicative of *α*-crystals. In other words, the LC-mesophase only partly transforms to *α*-crystals. Finally, on cooling at 1000 K·s^{-1}, the POM micrograph reveals a distinct Schlieren texture,[69–72] similar to that observed after quenching in ice-water, shown in Fig. 13. The Schlieren texture observed in PBN is characterized by the presence of multiple disclination lines and point singularities, from which typically four brushes are originating.

VITRIFICATION AND COLD-CRYSTALLIZATION OF PBN

FSC allows quantitative determination of critical cooling conditions for suppressing crystallization and even crystal nucleation.[40] Both crystallization and LC-mesophase formation

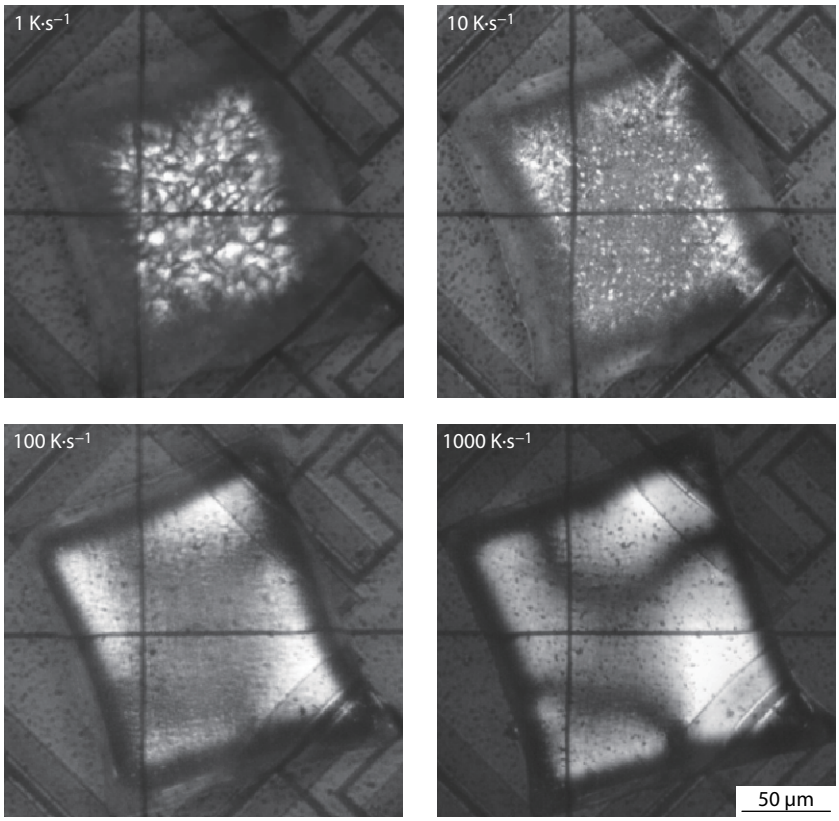

Fig. 12 POM reflection-mode micrographs of samples of PBN solidified on cooling at rates of 1, 10, 100, and 1000 K·s^{-1} in an FSC. (Adapted with permission from Ref. [35]; Copyright (2018) Elsevier.)

https://doi.org/10.1007/s10118-020-2354-5

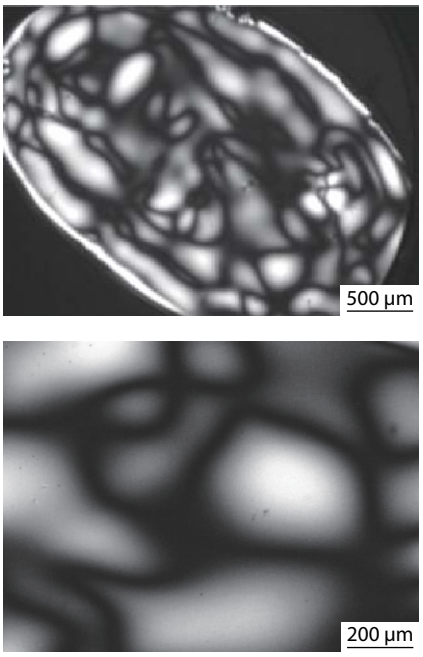

Fig. 13 POM micrographs of samples of PBN solidified by rapid cooling the melt from 290 °C by quenching into ice-water. (Adapted with permission from Ref. [66]; Copyright (2018) Elsevier.)

are completely suppressed when cooling the melt at a rate of 6000 K·s^{-1}, or faster, to below the glass transition temperature of the PBN melt. Fig. 14 shows an FSC curve recorded on heating fully amorphous PBN at a rate of 10000 K·s^{-1}, revealing the characteristic step-like increase of the heat capacity on devitrifying the glassy amorphous phase of PBN. As such, the onset of the glass transition occurred at about 42 °C and its midpoint was detected at 92 °C; the onset temperature agreed well with a former analysis performed using temperature-modulated DSC,[30] though the literature is not consistent regarding information about the glass transition temperatures, varying between 41 and 82 °C.[13,14,25,30,73,74]

Analysis of the enthalpy of cold-crystallization on heating fully amorphous PBN allows gaining knowledge about the formation of homogeneous crystal nuclei during prior cooling. Even if crystallization is suppressed on cooling faster than 6000 K·s^{-1}, there might be homogeneous crystal nuclei formed with their number detectable when permitting their growth in a subsequent thermal treatment, *e.g.*, when re-heating the material to above the glass transition temperature.[75–77] Systematic variation of the rate of cooling the quiescent melt revealed a critical cooling rate of 30000 K·s^{-1}, above which also the formation of nuclei is inhibited.[40]

With the availability of fully amorphous and glassy PBN, it is possible to study the structure formation on heating, that is, after devitrification of the glass. Systematic variation of the heating rate allows determination of a critical heating rate of 7000 K·s^{-1}, above which any ordering is suppressed on heating the melt to above the equilibrium melting temperature of the crystal polymorph of highest thermodynamic stability.[40] Worth noting is that the critical rates of cooling and heating the supercooled melt through the temperature range of possible ordering, that is, between the glass transition temperature and equilibrium melting temperature, are almost identical, being 6000 and 7000 K·s^{-1}, respectively. Slower heating at 1000 K·s^{-1} permits ordering and crystallization, as documented with the FSC curve and POM images of Fig. 15.[39] The equilibrium melt of PBN was cooled at a rate of 5000 K·s^{-1} to below the glass transition temperature, which yielded an almost completely amorphous sample. The corresponding featureless POM micrograph of glassy PBN, as positioned on the FSC sensor, is shown with the top left image. Heating the glass causes its devitrification at the glass transition temperature, which immediately allows exothermic LC-mesophase formation at a temperature slightly higher than 100 °C, followed by transformation of the mesophase into *α*-crystals close to 200 °C, and final melting of the *α*-crystals at around 230 °C. The formation of LC-phase is connected with the appearance of its characteristic Schlieren texture in POM, which, however, is not affected by the subsequent crystallization process at slightly higher temperature. The initially formed

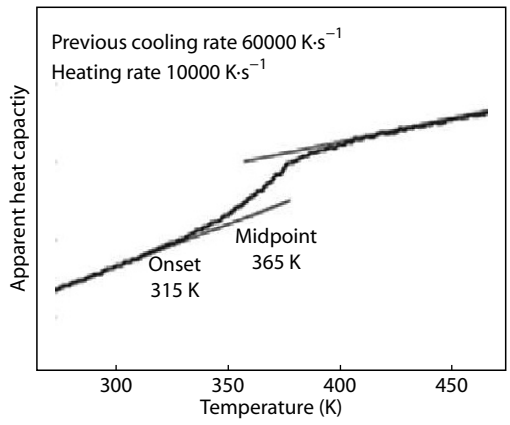

Fig. 14 FSC curve measured on heating PBN at a rate of 10000 K·s^{-1}. Prior heating, the material was vitrified using a cooling rate of 60000 K·s^{-1}. (Adapted with permission from Ref. [40]; Copyright (2015) Elsevier.)

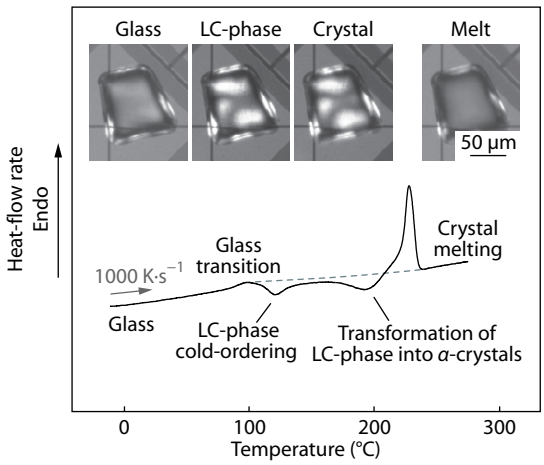

Fig. 15 FSC heating curve of PBN solidified on cooling at 5000 K·s^{-1}, recorded at a rate of 1000 K·s^{-1}. Inset: POM micrographs collected during heating initially almost fully amorphous PBN at a rate of 1 K·s^{-1}. Further explanation is available in the text. (Adapted with permission from Ref. [39]; Copyright (2018) Elsevier)

https://doi.org/10.1007/s10118-020-2354-5

texture is preserved until final melting occurs, suggesting that the LC-mesophase domains serve as an efficient precursor for the crystallization, proving the step-like sequence according to Ostwald's rule of stages. This observation is in agreement with the POM micrograph obtained on cooling the melt at a rate of 100 K·s^{-1} (see Fig. 12, bottom left), causing a similar two-step crystallization process, and preservation of the initially formed micrometer scale structure as observed after LC-mesophase formation.

Needless to say, the exact transition temperatures as well as the degree of completion of both transitions, LC-mesophase formation from the supercooled melt and crystals from the LC-mesophase, depend on the heating rate since they are kinetically controlled. For example, slow heating of the LC-mesophase at 4 K·min^{-1} allows formation of *α*-crystals well below 100 °C.[30] Fast heating of the LC-mesophase at 2000 K·s^{-1}, in contrast, suppresses the rather slow *α*-crystal-formation process and allows analysis of its disordering.[66]

CONCLUSIONS AND PERSPECTIVES

Poly(butylene 2,6-naphthalate) (PBN) is an engineering polyester displaying rich polymorphic behaviors, which include two different crystalline modifications and a liquid crystalline smectic mesophase. The various structures can be obtained by tailoring the temperature history, as they exhibit different thermal stability and formation kinetics.

Melt-crystallization at low or moderate supercoolings leads to the competitive growth of *β*′- and *α*-crystals, with the latter prevailing at lower crystallization temperatures. When the supercooling is further increased, the isotropic PBN melt transforms into a smectic liquid crystalline phase. This mesophase can subsequently turn into the more stable *α*-crystalline phase, in agreement with the well-known Ostwald's rule of stages. At non-isothermal solidification at high rates (*e.g.*, 1000 K·s^{-1}), this second transformation might be inhibited, leading to a smectic glass, while rates higher than 6000 K·s^{-1} are required to bypass liquid-crystallization from the melt and obtain a fully amorphous glass.

This review article provides an overview on the complex crystallization behavior of PBN, with particular attention to structural morphological and kinetic aspects of the different observed transitions. Due to the relatively high crystallization rate of this polymer, much information can only be derived thanks to recently available experimental techniques, such as fast scanning chip calorimetry and the use of synchrotron X-rays. Several issues deserve further investigations, and might enable interesting application of this peculiar semicrystalline polymer. For example, while several studies on PBN copolymers have been reported,[1,13,14,16,18,19,28,29,78,79] further variation of the type and content of co-units and molecular variables like the molar mass can be explored. Moreover, the effects of heterogeneous nucleation on the various transitions and the structuring in processing conditions, such as injection molding or fiber spinning, are presently unexplored. As such, we hope that this work will stimulate further research, and lead to a more comprehensive understanding of PBN crystallization.

ACKNOWLEDGMENTS

Q. D. acknowledges financial support from the China Scholarship Council (CSC), for performing research at the Martin Luther University Halle-Wittenberg (Germany). R. A. and Q. D. acknowledge financial support from Sino-German Center for Research Promotion (GZ 1514).

REFERENCES

1 Karayannidis, G. P.; Papageorgiou, G. Z.; Bikiaris, D. N; Tourasanidis, E. V. Synthesis and thermal behaviour of poly(ethylene-*co*-butylene naphthalene-2,6-dicarboxylate)s. *Polymer* **1998**, *39*, 4129–4134.
2 Jeong, Y. G.; Jo, W. H.; Lee, S. C. Synthesis and crystallization behavior of poly(*m*-methylene 2,6-naphthalate-*co*-1,4-cyclohexylenedimethylene 2,6-naphthalate) copolymers. *Macromolecules* **2003**, *36*, 4051–4059.
3 Soccio, M.; Finelli, L.; Lotti, N.; Siracusa, V.; Ezquerra, T. A.; Munari, A. Novel ethero atoms containing polyesters based on 2,6-naphthalendicarboxylic acid: a comparative study with poly(butylene naphthalate). *J. Polym. Sci., Part B: Polym. Phys.* **2007**, *45*, 1694–1703.
4 Hubbard, P.; Brittain, W. J.; Simonsick, W. J.; Ross, C. W. Synthesis and ring-opening polymerization of poly(alkylene 2,6-naphthalenedicarboxylate) cyclic oligomers. *Macromolecules* **1996**, *29*, 8304–8307.
5 https://www.teijin.com/products/resin/pbn/
6 Soccio, M.; Nogales, A.; García-Gutierrez, M. C.; Lotti. N.; Munari, A.; Ezquerra, T. A. Origin of the subglass dynamics in aromatic polyesters by labeling the dielectric relaxation with ethero atoms. *Macromolecules* **2008**, *41*, 2651–2655.
7 Mija, et al. **2018**, U.S. Pat., US2018/03051A1
8 https://marketdesk.us/report/global-polybutylene-naphthalate-resin-pbn-resin-market-pr/66961/#details
9 Wang, C. S.; Lin, C. H. On the miscibility and transesterification of poly(butylene naphthalate) with a novel phosphorus containing polyester. *Polymer* **2000**, *41*, 4029–4037.
10 Yoon, K. H.; Lee, S. C.; Park, O. O. Thermal properties of poly(ethylene 2,6-naphthalate) and poly(butylene 2,6-naphthalate) blends. *Polym. J.* **1994**, *26*, 816–821.
11 Dangseeyun, N.; Supaphol, P.; Nithitanakul, M. Thermal, crystallization, and rheological characteristics of poly(trimethylene terephthalate)/poly(butylene terephthalate) blends. *Polym. Test.* **2004**, *23*, 187–194.
12 Lin, C. H.; Wang, C. S. Miscibility of poly(etherimide) and poly(butylene naphthalate) blends. *Polym. Bull.* **2001**, *46*, 191–196.
13 Lee, S. C.; Yoon, K. H.; Kim, J. H. Crystallization kinetics of poly(butylene 2,6-naphthalate) and its copolyesters. *Polym. J.* **1997**, *29*, 1–6.
14 Papageorgiou, G. Z.; Karayannidis, G. P. Multiple melting behaviour of poly(ethylene-*co*-butylene naphthalene-2,6-dicarboxylate)s. *Polymer* **1999**, *40*, 5325–5332.
15 Papageorgiou, G. Z.; Karayannidis, G. P. Observations during crystallisation of poly(ethylene-*co*-butylene naphthalene-2,6-dicarboxylate)s. *Polymer* **2001**, *42*, 8197–8205.
16 Papageorgiou, G. Z.; Karayannidis, G. P.; Bikiaris, D. N.; Stergiou, A.; Litsardakis, G.; Makridis, S. S. Wide-angle X-ray diffraction and differential scanning calorimetry study of the crystallization of poly(ethylene naphthalate), poly(butylene naphthalate), and their copolymers. *J. Polym. Sci., Part B: Polym. Phys.* **2004**, *42*, 843–860.
17 Papageorgiou, D. G.; Bikiaris, D. N.; Papageorgiou, G. Z. Synthesis and controlled crystallization of *in situ* prepared poly(butylene-

2,6-naphthalate) nanocomposites. *Cryst. Eng. Comm.* **2018**, *20*, 3590–3600.
18 Soccio, M.; Gazzano, M.; Lotti, N.; Finelli, L.; Munari, A. Copolymerization: a new tool to selectively induce poly(butylene naphthalate) crystal form. *J. Polym. Sci., Part B: Polym. Phys.* **2009**, *47*, 1356–1367.
19 Soccio, M.; Gazzano, M.; Lotti, N.; Finelli, L.; Munari, A. Synthesis and characterization of novel random copolymers based on PBN: influence of thiodiethylene naphthalate co-units on its polymorphic behaviour. *Polymer* **2010**, *51*, 192–200.
20 Yokouchi, M.; Sakakibara, Y.; Chatani, Y.; Tadokoro, H.; Tanaka, T.; Yoda, K. Structures of two crystalline forms of poly(butylene terephthalate) and reversible transition between them by mechanical deformation. *Macromolecules* **1976**, *9*, 266–273.
21 Watanabe, H. Stretching and structure of polybutylene-naphthalene-2,6-dicarboxylate films. *Kobunshi. Ronbunshu.* **1976**, *33*, 229–237.
22 Koyano, H.; Yamamoto, Y.; Saito, Y.; Yamanobe, T.; Komoto, T. Crystal structure of poly(butylene-2,6-naphthalate). *Polymer* **1998**, *39*, 4385–4391.
23 Chiba, T.; Asai, S.; Xu, W.; Sumita, M. Analysis of crystallization behavior and crystal modifications of poly(butylene-2,6-naphthalene dicarboxylate). *J. Polym. Sci., Part B: Polym. Phys.* **1999**, *37*, 561–574.
24 Ju, M. Y.; Huang, J. M.; Chang, F. C. Crystal polymorphism of poly(butylene-2,6-naphthalate) prepared by thermal treatments. *Polymer* **2002**, *43*, 2065–2074.
25 Yamanobe, T.; Matsuda, H.; Imai, K.; Hirata, A.; Mori, S.; Komoto, T. Structure and physical properties of naphthalene containing polyesters. I. Structure of poly(butylene 2,6-naphthalate) and poly(ethylene 2,6-naphthalate) as studied by solid state NMR spectroscopy. *Polym. J.* **1996**, *28*, 177–181.
26 Tonelli, A. E. The conformations of poly(butylene-terephthalate) and poly(butylene-2,6-naphthalate) chains in their α and β crystalline polymorphs. *Polymer* **2002**, *43*, 6069–6072.
27 Milani, A. A revisitation of the polymorphism of poly(butylene-2,6-naphthalate) from periodic first-principles calculations. *Polymer* **2014**, *55*, 3729–3735.
28 Soccio, M.; Lotti, N.; Finelli, L.; Munari, A. Equilibrium melting temperature and crystallization kinetics of α- and β'-PBN crystal forms. *Polym. J.* **2012**, *44*, 174–180.
29 Jeong, Y. G.; Jo, W. H.; Lee, S. C. Cocrystallization behavior of poly(butylene terephthalate-*co*-butylene 2,6-naphthalate) random copolymers. *Macromolecules* **2000**, *33*, 9705–9711.
30 Konishi, T.; Nishida, K.; Matsuba, G.; Kanaya, T. Mesomorphic phase of poly(butylene-2,6-naphthalate). *Macromolecules* **2008**, *41*, 3157–3161.
31 Tokita, M.; Watanabe, J. Several interesting fields exploited through understanding of polymeric effects on liquid crystals of main-chain polyesters. *Polym. J.* **2006**, *38*, 611–638.
32 Tokita, M.; Osada, K.; Watanabe, J. Thermotropic liquid crystals of main-chain polyesters having a mesogenic 4,4′-biphenyldicarboxylate unit XI Smectic liquid crystalline glass. *Polym. J.* **1998**, *30*, 589–595.
33 Wunderlich, B. A classification of molecules, phases, and transitions as recognized by thermal analysis. *Thermochim. Acta* **1999**, *340*, 37–52.
34 Ju, M. Y.; Chang, F. C. Multiple melting behavior of poly(butylene-2,6-naphthalate). *Polymer* **2001**, *42*, 5037–5045.
35 Ding, Q.; Jehnichen, D.; Göbel, M.; Soccio, M.; Lotti, N.; Cavallo, D.; Androsch, R. Smectic liquid crystal Schlieren texture in rapidly cooled poly(butylene naphthalate). *Eur. Polym. J.* **2018**, *101*, 90–95.
36 Gazzano, M.; Soccio, M.; Lotti, N.; Finelli, L.; Munari, A. Crystallization kinetics, melting behavior, and RAP of novel etheroatom containing naphthyl polyesters. *J. Therm. Anal. Calorim.* **2012**, *110*, 907–915.
37 Ostwald, W. Studien über die Bildung und Umwandlung fester Körper. *Phys. Chem.* **1887**, *22*, 286–330.
38 Threlfall, T. Structural and thermodynamic explanations of Ostwald's rule. *Org. Process Res. Dev.* **2003**, *7*, 1017–1027.
39 Androsch, R.; Soccio, M.; Lotti, N.; Cavallo, D.; Schick, C. Cold-crystallization of poly(butylene 2,6-naphthalate) following Ostwald's rule of stages. *Thermochim. Acta* **2018**, *670*, 71–75.
40 Nishida, K.; Zhuravlev, E.; Yang, B.; Schick, C.; Shiraishi, Y.; Kanaya, T. Vitrification and crystallization of poly(butylene-2,6-naphthalate). *Thermochim. Acta* **2015**, *603*, 110–115.
41 Bernstein, J. *Polymorphism in molecular crystals*. Oxford University Press, New York, **2002**.
42 Chung, S. Y.; Kim, Y. M.; Kim, J. G.; Kim, Y. J. Multiphase transformation and Ostwald's rule of stages during crystallization of a metal phosphate. *Nat. Phys.* **2009**, *5*, 68–73.
43 Gliko, O.; Neumaier, N.; Pan, W.; Haase, I.; Fischer, M.; Bacher, A.; Weinkauf, S.; Vekilov, P. G. A metastable prerequisite for the growth of lumazine synthase crystals. *J. Am. Chem. Soc.* **2005**, *127*, 3433–3438.
44 Chung, S.; Shin, S. H.; Bertozzi, C. R.; De Yoreo, J. J. Self-catalyzed growth of S layers *via* an amorphous-to-crystalline transition limited by folding kinetics. *Proc. Natl. Acad. Sci.* **2010**, *107*, 16536–16541.
45 Auer, S.; Frenkel, D. Prediction of absolute crystal-nucleation rate in hard-sphere colloids. *Nature* **2001**, *409*, 1020–1023.
46 Zhang, T. H.; Liu, X. Y. Nucleation: what happens at the initial stage? *Angew. Chem. Int. Ed.* **2009**, *48*, 1308–1312.
47 Pérez-Manzano, J.; Fernández-Blázquez, J. P.; Bello, A.; Pérez, E. Liquid-crystalline copolymers of bibenzoate and terephthalate units. *Polym. Bull.* **2006**, *56*, 571–577.
48 Hu, Y. S.; Hiltner, A.; Baer, E. Solid state structure and oxygen transport properties of copolyesters based on smectic poly(hexamethylene 4,4′-bibenzoate). *Polymer* **2006**, *47*, 2423–2433.
49 Fernández-Blázquez, J. P.; Pérez-Manzano, J.; Bello, A.; Pérez, E. The two crystallization modes of mesophase forming polymers. *Macromolecules* **2007**, *40*, 1775–1778.
50 Heck, B.; Perez, E.; Strobl, G. Two competing crystallization modes in a smectogenic polyester. *Macromolecules* **2010**, *43*, 4172–4183.
51 Jin, J. I.; Kang, C. S. Thermotropic main chain polyesters. *Prog. Polym. Sci.* **1997**, *22*, 937–973.
52 Watanabe, J.; Hayashi, M. Thermotropic liquid crystals of polyesters having a mesogenic p,p′-bibenzoate unit. 1. Smectic A mesophase properties of polyesters composed of p,p'-bibenzoic acid and alkylene glycols. *Macromolecules* **1988**, *21*, 278–280.
53 Watanabe, J.; Hayashi, M. Thermotropic liquid crystals of polyesters having a mesogenic p,p'-bibenzoate unit. 2. X-ray study on smectic mesophase structures of BB-5 and BB-6. *Macromolecules* **1989**, *22*, 4083–4088.
54 Bello, A.; Pereña, J. M.; Pérez, E.; Benavente, R. Thermotropic liquid crystal polyesters derived from 4,4′-biphenyldicarboxylic acid and oxyalkylene spacers. *Macromol. Symp.* **1994**, *84*, 297–306.
55 Chen, D.; Zachmann, H. G. Glass transition temperature of copolyesters of PET, PEN and PHB as determined by dynamic mechanical analysis. *Polymer* **1991**, *32*, 1612–1621.
56 Watanabe, J.; Hasayashi, M.; Nakata, Y.; Niori, T.; Tokita, M. Smectic liquid crystals in main-chain polymers. *Prog. Polym. Sci.* **1997**, *22*, 1053–1087.
57 Martínez-Gómez, A.; Encinar, M.; Fernández-Blázquez, J. P.; Rubio, R. G.; Pérez, E. *Liquid crystalline polymers*. Springer, Berlin, **2016**, p. 453–476.

https://doi.org/10.1007/s10118-020-2354-5

58 Keller, A.; Hikosaka, M.; Rastogi, S.; Toda, A.; Barham, P. J.; Goldbeck-Wood, G. An approach to the formation and growth of new phases with application to polymer crystallization: effect of finite size, metastability, and Ostwald's rule of stages. *J. Mater. Sci.* **1994**, *29*, 2579–2604.

59 Keller, A.; Cheng, S. Z. D. The role of metastability in polymer phase transitions. *Polymer* **1998**, *39*, 4461–4487.

60 Cheng, S. Z. D.; Zhu, L.; Y. Li, C.; Honigfort, P. S.; Keller, A. Size effect of metastable states on semicrystalline polymer structures and morphologies. *Thermochim. Acta* **1999**, *332*, 105–113.

61 Cheng, S. Z. D. *Phase transitions in polymers*. Elsevier, Amsterdam, **2008**.

62 Cavallo, D.; Mileva, D.; Portale, G.; Zhang, L.; Balzano, L.; Alfonso, G. C.; Androsch, R. Mesophase-mediated crystallization of poly(butylene-2,6-naphthalate): an example of Ostwald's rule of stages. *ACS Macro Lett.* **2012**, *1*, 1051–1055.

63 Achilias, D. S.; Papageorgiou, G. Z.; Karayannidis, G. P. Evaluation of the isoconversional approach to estimating the Hoffman-Lauritzen parameters from the overall rates of non-isothermal crystallization of polymers. *Macromol. Chem. Phys.* **2005**, *206*, 1511–1519.

64 Schick, C.; Mathot, V. *Fast scanning calorimetry*. Springer, Berlin, **2016**.

65 Toda, A.; Androsch, R.; Schick, C. Insights into polymer crystallization and melting from fast scanning chip calorimetry. *Polymer* **2016**, *91*, 239–263.

66 Androsch, R.; Soccio, M.; Lotti, N.; Jehnichen, D.; Göbel, M.; Schick, C. Enthalpy of formation and disordering temperature of transient monotropic liquid crystals of poly(butylene 2,6-naphthalate). *Polymer* **2018**, *158*, 77–82.

67 Cheng, S. Z. *Phase transitions in polymers: the role of metastable states*. Elsevier, Amsterdam, **2008**, p. 25.

68 Singh, S. *Liquid crystals fundamentals*. World Scientific, New Jersey, **2002**, p. 58

69 de Gennes, P. G.; Prost, J. *The physics of liquid crystals*. Oxford University Press, New York, **1993**, p. 58

70 Sackmann, H.; Demus, D. The polymorphism of liquid crystals. *Mol. Cryst.* **1966**, *2*, 81–102.

71 Nehring, J.; Saupe, A. On the schlieren texture in nematic and smectic liquid crystals. *J. Chem. Soc., Faraday Trans. 2: Mol. Chem. Phys.* **1972**, *68*, 1–15.

72 Demus, D. Schlieren textures in smectic liquid crystals. *Kristall und Technik* **1975**, *10*, 933–946.

73 Jakeways, R.; Ward, I. M.; Wilding, M. A.; Hall, I. H.; Desborough, I. J.; Pass, M. G. Crystal deformation in aromatic polyesters. *J. Polym. Sci., Part B: Polym. Phys.* **1975**, *13*, 799–813.

74 Sun, Y. M.; Wang, C. S. Novel copolyesters containing naphthalene structure. I. From bis(hydroxyalkyl)naphthalate and bis[4-(2-hydroxyethoxy)aryl] compounds. *J. Polym. Sci., Part A: Polym. Chem.* **1996**, *34*, 1783–1792.

75 Zhuravlev, E.; Schmelzer, J. W.; Abyzov, A. S.; Fokin, V. M.; Androsch, R.; Schick, C. Experimental test of Tammann's nuclei development approach in crystallization of macromolecules. *Cryst. Growth Des.* **2015**, *15*, 786–798.

76 Androsch, R.; Iqbal, H. N.; Schick, C. Non-isothermal crystal nucleation of poly(L-lactic acid). *Polymer* **2015**, *81*, 151–158.

77 Salmerón Sánchez, M.; Mathot, V. B.; Vanden Poel, G.; Gómez Ribelles, J. L. Effect of the cooling rate on the nucleation kinetics of poly(L-lactic acid) and its influence on morphology. *Macromolecules* **2007**, *40*, 7989–7997.

78 Papageorgiou, G. Z.; Tsanaktsis, V.; Bikiaris, D. N. Crystallization of poly(butylene-2,6-naphthalate-*co*-butylene adipate) copolymers: regulating crystal modification of the polymorphic parent homopolymers and biodegradation. *Cryst. Eng. Commun.* **2014**, *16*, 7963–7978.

79 Ding; Q.; Soccio, M.; Lotti, N.; Mahmood, N.; Cavallo, D.; Androsch, R. Crystallization of poly(butylene 2,6-naphthalate) containing diethylene 2,6-naphthalate constitutional defects. *Polym. Crys.* **2019**.

https://doi.org/10.1007/s10118-020-2354-5